Phylogenomics Illuminates the Evolutionary History of Wild Silkmoths in Space and Time (Lepidoptera: Saturniidae)

RUNNING HEAD: PHYLOGENY AND BIOGEOGRAPHY OF SATURNIIDAE MOTHS

Rodolphe Rougerie[1*£], Astrid Cruaud[2£], Pierre Arnal[1,2£], Liliana Ballesteros-Mejia[1,3], Fabien L. Condamine[4], Thibaud Decaëns[5], Marianne Elias[1], Delphine Gey[6,7], Paul D. N. Hebert[8], Ian J. Kitching[9], Sébastien Lavergne[10], Carlos Lopez-Vaamonde[11,12], Jérôme Murienne[13], Yves Cuenot[13], Sabine Nidelet[2], Jean-Yves Rasplus[2]

[1] *Institut de Systématique, Évolution, Biodiversité (ISYEB), Muséum national d'Histoire naturelle, CNRS, EPHE, Sorbonne Université, Université des Antilles, Paris, France (rodolphe.rougerie@mnhn.fr)*

[2] *Centre de Biologie pour la Gestion des Populations (CBGP), INRAE, CIRAD, IRD, Montpellier SupAgro, Université de Montpellier, Montpellier, France*

[3] *CESAB, Centre de Synthèse et d'Analyse sur la Biodiversité, Montpellier, France*

[4] *Institut des Sciences de l'Évolution de Montpellier (ISEM), CNRS, Université de Montpellier, Montpellier, France*

[5] *Centre d'Écologie Fonctionnelle et Évolutive (CEFE), Université de Montpellier, CNRS, EPHE, IRD, Montpellier, France*

[6] *Service de Systématique Moléculaire, UAR 2700 2AD, Muséum national d'Histoire naturelle, Paris, France*

[7] *Molécules de Communication et Adaptation des Microorganismes (MCAM), Muséum national d'Histoire naturelle, CNRS, Paris, France*

[8] *Center for Biodiversity Genomics, University of Guelph, Guelph, Canada*

[9] *Department of Life Sciences, Natural History Museum, London, United Kingdom*

[10] *Université Grenoble Alpes, CNRS, Université Savoie Mont Blanc, Laboratoire d'Écologie Alpine (LECA), Grenoble, France*

[11] *Institut de Recherche sur la Biologie de l'Insecte, UMR7261 CNRS - Université de Tours, France*

[12] *INRAE, UR633, Zoologie Forestière, F-45075 Orléans, France*

[13] *Laboratoire Évolution et Diversité Biologique (EDB UMR5174), Université Toulouse 3 Paul Sabatier, CNRS, IRD, Toulouse, France*

[*]corresponding author

[£]equal contributors

ABSTRACT

Wild silkmoths (Saturniidae) are one of the most emblematic and most studied families of moths. Yet, the absence of a robust phylogenetic framework based on a comprehensive taxonomic sampling impedes our understanding of their evolutionary history. We analyzed 1,024 ultraconserved elements (UCEs) and their flanking regions to infer the relationships among 338 species of Saturniidae representing all described subfamilies, tribes, and genera. We investigated systematic biases in genomic data and performed dating and historical biogeographic analyses to reconstruct the evolutionary history of wild silkmoths in space and time. Using Gene Genealogy Interrogation, we showed that saturation of nucleotide sequence data blurred our understanding of early divergences and first biogeographic events. Our analyses support a Neotropical origin of saturniids, shortly after the Cretaceous-Paleogene extinction event (*ca* 64.0 [stem] - 52.0 [crown] Ma), and two independent colonization events of the Old World during the Eocene, presumably through the Bering Land Bridge. Early divergences strongly shaped the distribution of extant subfamilies as they showed very limited mobility across biogeographical regions, except for Saturniinae, a subfamily now present on all continents but Antarctica. Overall, our results provide a framework for in-depth investigations into the spatial and temporal dynamics of all saturniid lineages and for the integration of their evolutionary history into further global studies of biodiversity and conservation. Rather unexpectedly for a taxonomically well-known family such as Saturniidae, the proper alignment of taxonomic divisions and ranks with our phylogenetic results leads us to propose substantial rearrangements of the family classification, including the description of one new subfamily and two new tribes.

KEYWORDS: Historical Biogeography; Moths; Phylogenomics; Saturation; Taxonomy; Ultra-Conserved Elements

Thanks to generations of naturalists, moths in the family Saturniidae – also known as wild silkmoths – are now among the best documented insects, particularly because of their spectacular variation in size and form in both adult and immature stages. The family encompasses some of the largest (e.g., *Coscinocera hercules* and *Attacus* species that reach 30cm wingspan) and most emblematic moths (e.g., the moon moths, *Actias* species and the comet moth, *Argema mittrei*). Wild silkmoths also bear importance to humans for silk production (Kundu et al. 2012, Dong et al. 2015), as a food resource (Fogang Mba et al. 2019), and for health concern (Carrijo-Carvalho and Chudzinski-Tavassi 2007, Battisti et al. 2011, Ciminera et al. 2018). However, despite being one of the best-known families of Lepidoptera, a robust phylogenetic hypothesis of interrelationships among its genera based on extensive sampling is lacking. Saturniids are considered to be poor-dispersers, because of their large and short-lived non-feeding adults that represent an extreme case of capital-breeding organisms (Davis et al. 2016). These moths nonetheless managed to colonize and diversify on almost all continents, but the spatial and temporal dynamics of their evolutionary history remain largely unknown, for neither formal biogeographical analyses nor inferences from time trees have been drawn for the family.

Saturniidae comprise 3,454 species and 180 genera worldwide, classified into eight subfamilies and 11 tribes (Kitching et al. 2018). Five of these subfamilies (Arsenurinae, Ceratocampinae, Cercophaninae, Hemileucinae and Oxyteninae) are restricted to the New World and comprise 60% of the diversity of the family (>2,100 species). The subfamily Agliinae (5 species) occurs throughout the Palearctic region while most species of Salassinae (32 species) are in the Sino-Himalayan region with a few species in the East Palearctic and Oriental regions. Finally, the highly diversified Saturniinae (>1,000 species) are present in all biogeographical regions, except for polar and desertic regions. The family is considered monophyletic based on both morphological (Minet 1994) and molecular evidence (Regier et

al. 2008, Breinholt et al. 2018, Hamilton et al. 2019). A few studies have addressed higher-level relationships within the Saturniidae although with sparse taxon and often reduced gene sampling (Regier et al. 2008: 8 species, 7 subfamilies, 5 loci, Barber et al. 2015: 80 species, 8 subfamilies, 6 loci, Hamilton et al. 2019: 16 species, 8 subfamilies, 650 loci). Nevertheless, a consensus has emerged that the Neotropical Oxyteninae is sister to all other Saturniidae while the Cercophaninae is the second earliest-diverging subfamily. The remaining lineages are divided into two large clades, a Neotropical clade that includes three subfamilies (Arsenurinae + Ceratocampinae + Hemileucinae), and an old-world clade composed of Salassinae as sister to Saturniinae. However, the position of the eighth subfamily – the palearctic Agliinae – remains contentious. In recent phylogenomic analyses based on anchored hybrid enrichment (Rubin et al. 2018, Hamilton et al. 2019), Agliinae is recovered as sister to the old-world clade, but with low support, rather than as sister to the new-world clade as found in studies based on Sanger sequencing of a few loci and with low support as well (Regier et al. 2008, Barber et al. 2015, Rubinoff and Doorenweerd 2020). Beside this uncertainty, previous studies have also raised questions regarding the placement of certain taxa, such as the genus *Rhodinia* which has been placed as a member of the tribes Saturniini (Regier et al. 2002) or Attacini (Rubin et al 2018; Chen et al. 2021), or poorly known genera such as the African *Eosia* and *Eochroa* – doubtfully placed, respectively, in Micragonini and Bunaeini tribes within Saturniinae (Oberprieler and Nässig 1994), or *Hirpida* and *Catharisa* of unclear affinities within Hemileucinae (Michener 1952, Lemaire 2002). The latter is the most speciose subfamily with more than 1,600 species in 55 genera, of which just eleven have been included in a formal phylogenetic analysis (Barber et al 2015). Furthermore, although both morphology and molecules have revealed the paraphyly of Urotini with respect to Afrotropical Bunaeini and Micragonini (Regier et al 2008, Rubin et al 2018), incomplete

taxon sampling led taxonomists to refrain from revising a classification recognized as unnatural for African Saturniidae (Oberprieler, 1997).

While genome-scale data can often help resolving phylogenetic relationships, they have proven frustrating when addressing difficult nodes within the Saturniidae, presumably because of the lack of signal associated with an old, rapid radiation (Hamilton et al. 2021) and of the increasing probability of observing conflicting signals between markers (Kumar et al. 2012). In particular, although these properties are still rarely thoroughly explored, heterogeneity in base composition and evolutionary rates of taxa and markers (e.g., Boussau et al. 2014, Romiguier et al. 2016, Bossert et al. 2017, Borowiec et al. 2019, Cruaud et al. 2021, Rasplus et al. 2021) as well as saturation (Borowiec 2019, Duchêne et al. 2021) were identified as major causes of analytical bias in phylogenomic analyses. These factors, in concert with limited taxon sampling, may, for instance, explain the poorly resolved placement of Agliinae within the Saturniidae (Hamilton et al. 2019) and constrain our understanding of the early evolutionary history of this family.

In this study, we present a new time-calibrated phylogeny of Saturniidae reconstructed with 1,024 ultraconserved elements (UCEs) and their flanking regions obtained from 338 species representing all described subfamilies, tribes, and genera of Saturniidae. We analyzed potential systematic bias in genomic data and used the best-supported phylogenomic hypothesis to (1) propose a revised classification of the family that reflects these inferred relationships, and (2) infer a timeline for the origin and dispersal patterns of the family through the estimation of its biogeographical history.

MATERIALS AND METHODS

Taxon Sampling

Our taxonomic sampling included 9.8% of all species of Saturniidae (338/3454) and representatives of all recognized subfamilies (8), tribes (11), and genera (180) (Kitching et al. 2018). Our samples also included representatives of all subgenera of *Psilopygida*, *Meroleuca*, *Gonimbrasia*, and *Antheraea*, and five of the six subgenera of *Hylesia* (Table S1). Sixteen outgroup species were used, including (1) ten species of Sphingidae, the sister family of Saturniidae (Hamilton et al. 2019), with representatives from all four of its subfamilies, and (2) six species from four other families of Bombycoidea (Brahmaeidae, Endromidae, Bombycidae and Eupterotidae).

Library Preparations and Sequencing

Samples were obtained from tissue collections at CBGP and MNHN, and from historical specimen collections at MNHN when necessary. DNA was extracted from thorax muscles or legs using the Qiagen DNeasy Blood and Tissue kit and following manufacturer's protocol with modifications detailed in Cruaud et al. (2019). Alternatively, we also used DNA extracts prepared for DNA barcoding studies at the Centre for Biodiversity Genomics (University of Guelph, Ontario, Canada) following the protocol in Ivanova et al. (2006). Library preparations followed Cruaud et al. (2019). Pools of 16 specimens made at equimolar ratio were enriched in 1,381 UCEs using the 14,363 baits designed by Faircloth (2017) (ordered as a myBaits UCE kit; Arbor Biosciences). Batches of 96 samples were sequenced on different flow cells of an Illumina MiSeq platform with a 2x250 pb paired-end sequencing.

Assembly of Data Sets into Loci, Data Set Cleaning

Filtering of raw data and assembly into loci followed Cruaud et al. (2019). Only UCEs that had a sequence from at least 50% of the samples were retained for analysis (n=1,024). Loci were aligned with MAFFT (*-linsi* option; Katoh and Standley 2013). Sites with more

than 50% gaps and sequences with more than 25% gaps were removed from each UCE using SEQTOOLS (package *PASTA*; Mirarab et al. 2015)). For all loci, two successive rounds of TreeShrink (Mai and Mirarab 2018) were performed to detect and remove abnormally long branches in individual gene trees, using the *per-species* mode and *b* parameter set to 20. Loci were realigned with MAFFT between and after the two rounds of TreeShrink; gene trees were inferred with IQ-TREE 2.0.6 (Minh et al. 2020) with the best fit model selected by ModelFinder (Kalyaanamoorthy et al. 2017).

Phylogenetic Analyses

UCEs were analyzed with concatenation (IQ-TREE 2.0.6) and tree reconciliation (ASTRAL-III, Zhang et al. 2018) approaches. For the concatenation approach, aligned UCEs were merged and the resulting data set was analyzed without (hereafter referred to as IQTREE-unpartitioned) and with partitions within the alignment. For the partitioned analysis, each UCE was first divided into one core and two flanking regions using the Sliding-Window Site Characteristics (SWSC) method (Tagliacollo et al. 2018). We then tested two partitioning schemes: (1) a partition that grouped all core regions and another that grouped all flanking regions (hereafter referred to as IQTREE-CoreVsFlanking); and (2) the best partitioning scheme inferred by PartitionFinder2 (Lanfear et al. 2017) that joins core and flanking regions under a similar evolutionary model (model selection = AICc; algorithm = rclusterf; branch lengths linked; hereafter referred to as IQTREE-PartitionFinder). Best-fit models for the unpartitioned data set and for all partitions were selected with the Bayesian Information Criterion (BIC) as implemented in ModelFinder (Kalyaanamoorthy et al. 2017). FreeRate models with up to ten categories of rates were included in tests for the unpartitioned data set and for partitions that grouped all core regions or all flanking regions, but only common substitution models were tested for the subsets identified by PartitionFinder. The candidate

tree set for all tree searches was composed of 98 parsimony trees + 1 BIONJ tree and only the 20 best initial trees were retained for NNI search. Node supports were assessed with ultrafast bootstrap (UFBoot) (Minh et al. 2013) with a minimum correlation coefficient set to 0.99 and 1,000 replicates of SH-aLRT tests (Guindon et al. 2010). UFBoot values ≥ 95 and SH-aLRT ≥ 80 were considered as strong support for a node. In addition, we computed gene (gCF) and site (sCF) concordance factors (Minh et al. 2020) with IQ-TREE.

For ASTRAL analyses, nodes in gene trees with UFBoot support lower than 50, 70, or 90 were collapsed following the approach of Zhu (2014, perl script AfterPhylo.pl) before reconciliation (trees are hereafter referred to as ASTRAL50, ASTRAL70 and ASTRAL90, respectively). Node supports for the ASTRAL trees were evaluated with local posterior probabilities (local PP). RF distances (Robinson and Foulds 1981) among recovered trees were calculated with RAxML-NG_v0.9.0 (Kozlov et al. 2019) and Approximately Unbiased (AU) tests (Shimodaira 2002) were performed with IQ-TREE (number of bootstrap replicates set to 20,000).

Analysis of Conflicting Topologies and Bias Exploration

Systematic biases were investigated with respect to influences from both loci and taxa. For analyses based on loci, Gene Genealogy Interrogation (GGI) (Arcila et al. 2017, Zhong and Betancur-R 2017, Betancur-R et al. 2019) was used to identify UCEs that supported each of the competing topologies. Each UCE was analyzed with IQ-TREE to infer trees using each of the competing topologies as multifurcating constraint trees (the structure of the backbone was fixed, but taxa within identified clades were free to move around). Per-site log-likelihood scores for all constrained trees were then calculated with RAxML-8.2.11 (Stamatakis 2014) and used to perform AU tests in CONSEL (Shimodaira and Hasegawa 2001). The program *makermt* in CONSEL was used to generate K = 10 sets of bootstrap replicates with each set

consisting of 100,000 replicates of the row sums. Properties of the UCEs that supported each topology were compared to detect whether significant differences could be identified between groups of UCEs and whether any topology could result from analytical bias. Two properties that are known to bias phylogenetic analyses, GC content (Romiguier and Roux 2017) and saturation (Philippe et al. 2001, Duchêne et al. 2021), were analyzed. GC content was calculated with AMAS (Borowiec 2016) and saturation (R squared of the linear regression of uncorrected p-distances against inferred distances in individual gene trees) was calculated following Borowiec et al. (2015). Results were analyzed in R (R Core Team 2018) using the packages *ggpubr* (Kassambara 2020) and *rich* (Rossi 2011).

For analyses based on taxa, GC content and long branch (LB) score heterogeneity were calculated for each taxon in each UCE and in the concatenated data set. GC content was calculated with AMAS and LB heterogeneity scores were calculated with TreSpEx (Struck 2014). In each tree, the per sample LB score measures how the patristic distance (PD) of a sample to all others deviates (as a percentage) from the average PD across all samples (Struck, 2014). The calculation of the heterogeneity in LB scores can therefore help to reveal possible Long Branch Attraction (LBA) artefacts (Bergsten 2005). Hierarchical clustering of taxa based on GC content and LB scores was performed with the R package *cluster* (Maechler et al. 2018).

Divergence Time Estimates

We estimated divergence times for Saturniidae with MCMCtree (Yang and Rannala 2006), using uniform distributions as calibration priors. A sphingid fossil (†*Mioclanis shanwangiana*) provided a minimum age for the crown of Smerinthinii set to 15.0 Ma (Zhang et al. 1994, Yang et al. 2007), while a maximum of 44.9 Ma was set following the maximum age estimate for Sphingidae in Kawahara et al. (2019). For secondary calibration, the

minimum and maximum bounds of four selected nodes were respectively set to the mean of minimum ages and the mean of maximum ages obtained by Kawahara et al. (2019) with different calibration schemes and relaxed-clock models: (1) root (crown Bombycoidea): 59.6-81.1 Ma; (2) crown Saturniidae + Sphingidae: 48.8-69.0 Ma; (3) crown Saturniidae: 35.1-52.5 Ma; and (4) crown Sphingidae: 29.6-44.9 Ma. Analyses were run with uncorrelated and correlated relaxed clock models. The IQ-TREE topology obtained with the 50% least saturated UCEs loci was used as input tree. Five data sets composed of 30,000 randomly selected sites (custom script) were used as input data to make computation tractable. Two chains were run for each data set, 20,000 generations were discarded as burnin, and chains were run for at least 2 million generations with sampling every 200 generations and until effective sample sizes of parameters reached at least 200 as reported by Tracer (Rambaut et al. 2018). Possible conflicts between priors and data were controlled by sampling directly from the prior of times and rates. Prior and posterior distributions were then compared in Tracer. Marginal densities of parameters obtained with different data sets were compared with Tracer. Posterior estimates obtained with the different chains were combined with LogCombiner 2.6.0 (Bouckaert et al. 2019).

Historical Biogeography

Species distributions were assigned as presence/absence to the nine following biogeographical areas: Neotropical, West Nearctic, East Nearctic, Afrotropical, Australasian, Madagascar, Oriental, West Palearctic, and East Palearctic (Table S2). Ancestral area estimations were performed using the R package *BioGeoBEARS 1.1.1* (Matzke 2014). The chronogram built with MCMCtree was used as input but only one specimen per genus/subgenus was included in the analysis and outgroups were removed to avoid artefacts (taxa were pruned from the chronogram with the R package *ape* (Paradis and Schliep 2018)).

Dispersal-Extinction-Cladogenesis (DEC; Ree and Smith 2008), BAYAREALIKE (Landis et al. 2013) and DIVALIKE (Ronquist 1997) models were used with and without considering the jump parameter for founder events (+*J*; Matzke 2014). Model selection was performed by considering statistical (AICc; Klaus and Matzke 2020, Matzke 2021) and non-statistical (i.e., biological and geographical) information (Ree and Sanmartin 2018). The maximum number of areas that a species could occupy was set to 5. To consider the main geological events that occurred during the diversification of Saturniidae, we defined five time periods with different dispersal rate scalers: (1) from the mean crown age of Saturniidae (ca. 52 Ma) to 34 Ma; (2) 34 to 23 Ma (Oligocene); (3) 23 to 14 Ma (early to mid-Miocene); (4) 14 to 5 Ma (mid to late Miocene); (5) 5 Ma to present. Dispersal rate matrices between areas and adjacency matrices are provided in Table S2.

RESULTS

Initial Data Set and Trees

The initial phylogenomic data set included sequence information for 354 taxa (338 species from 185 genera of Saturniidae + 16 outgroup species) and 1,024 UCEs representing 579,775 aligned bp (215,449 bp for core regions and 364,326 bp for flanking regions) of which 66.7% were parsimony informative (Table S3). PartitionFinder grouped the 3,072 core/flanking regions into 1,943 subsets. The six trees (IQTREE-unpartitioned, IQTREE-CoreVsFlanking, IQTREE-PartitionFinder, ASTRAL50, ASTRAL70, ASTRAL90) are shown in Figure S1. Relationships within Saturniidae inferred by IQTREE were well resolved with only 6-7% of the nodes receiving SH-aLRT/UFBoot scores below 100/100. IQ-TREE trees were considered as equally good explanations of the data set (AU test *P*-value > 0.05; Table S3), regardless of the partitioning scheme.

The differences between IQ-TREE topologies (RF pairwise distances 4-8; Table S3) were located in a few poorly supported regions of the topology (within Bunaeini and Arsenurinae). Except for 8-10% of the nodes, local PP were above 0.99 in ASTRAL trees. The differences between ASTRAL topologies (RF pairwise distances 6-14; Table S3) were restricted to parts that were poorly supported. Depending on the pairs of topologies compared, from 19 to 24 clades were observed in IQ-TREE trees but not in ASTRAL trees and vice versa. All conflicts (but one, see next section) were either unsupported in IQ-TREE trees, ASTRAL trees, or in both types of trees.

Saturniidae was recovered monophyletic with maximal node support in all analyses. All subfamilies were recovered as monophyletic with strong support except Hemileucinae which was polyphyletic with *Hirpida* + *Hirpsinjaevia* well separated from other species. The Oxyteninae and Cercophaninae formed a grade sister to all other saturniids. Except for Agliinae and *Hirpida* + *Hirpsinjaevia* (Fig. 1; see next section), relationships among the main lineages were strongly supported with Arsenurinae recovered as sister to Ceratocampinae + Hemileucinae (excluding *Hirpida* + *Hirpsinjaevia*) and Salassinae recovered as sister to Saturniinae. All but five tribes (Hemileucini, Urotini, Micragonini, Saturniini, Bunaeini) were recovered as monophyletic with strong support. Finally, 95 (92%) of the 103 genera represented by multiple species were recovered as monophyletic. The six genera *Automeris*, *Eacles*, *Ludia*, *Neodiphthera*, and *Pseudodirphia* were problematic as they were rendered paraphyletic, respectively, by *Eubergioides*, *Catharisa*, *Vegetia*, *Pararhodia*, and *Kentroleuca*. Two genera (*Gonimbrasia*, *Molippa*) appeared polyphyletic while *Syssphinx* was recovered as a grade that also included the North American *Dryocampa* and *Anisota*.

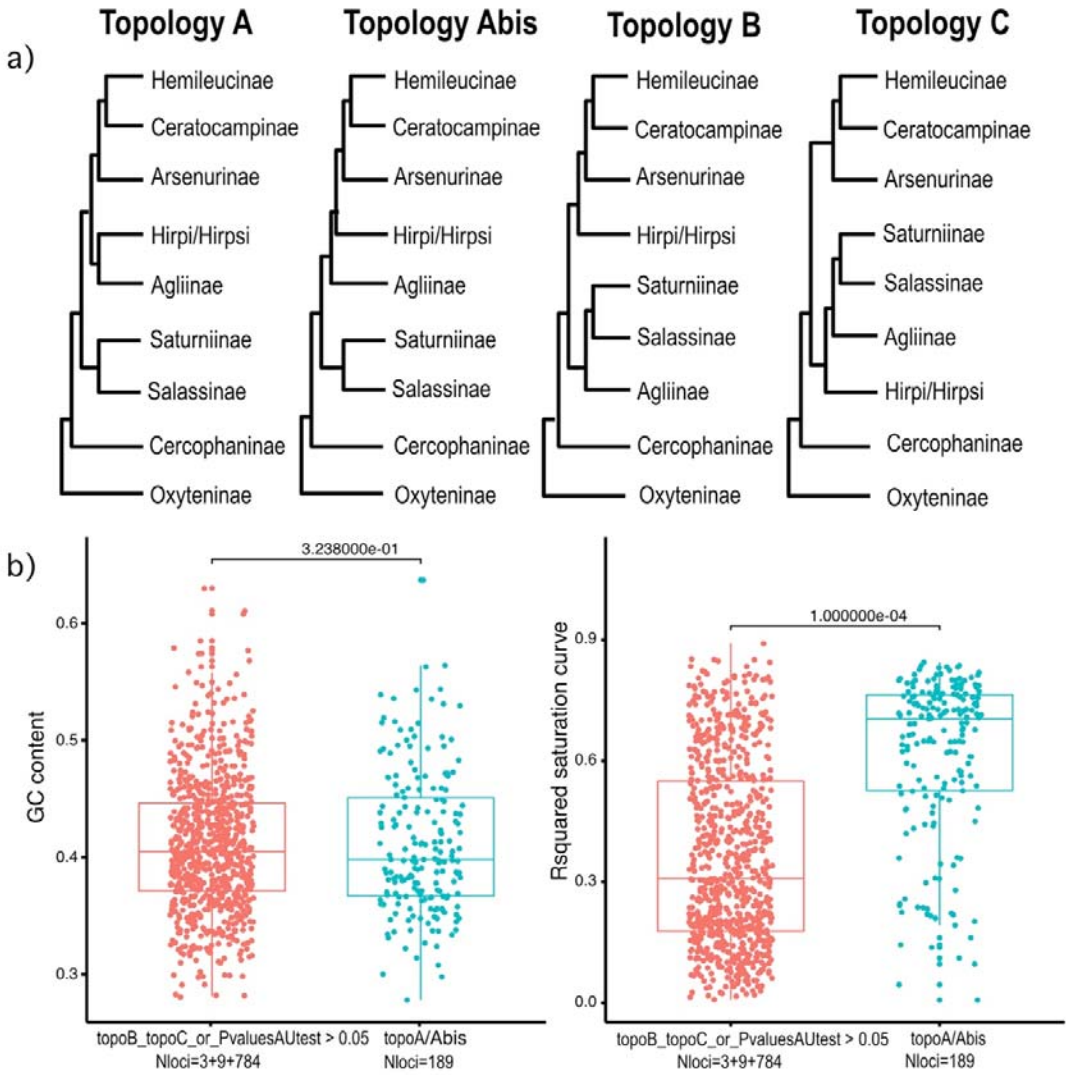

Figure 1. Conflicting topologies observed after analysis of the initial data set (a) and results of the gene genealogy interrogation (GGI) approach (b). In panel (a), topology *A* is supported by IQ-TREE analyses; *Abis* is supported by ASTRAL90; *B* is supported by ASTRAL70 and *C* is supported by ASTRAL50. All corresponding trees are available in Figure S1. In simplified topologies, Hemileucinae is used for Hemileucinae minus *Hirpida* and *Hirpsinjaevia* and Hirpi/Hirpsi stands for *Hirpida* + *Hirpsinjaevia*. For the GGI approach, Hemileucinae (minus *Hirpida* and *Hirpsinjaevia*) + Ceratocampinae + Arsenurinae; Saturniinae + Salassinae; *Hirpida* + *Hirpsinjaevia* and Agliinae were considered as different clades and trees were inferred using each of the competing topologies as multifurcating constraint trees. The structure of the backbone was fixed, but taxa within clades were

free to move around. Topology *A* was considered equivalent to *Abis* as we focused on sister taxa relationships of Agliinae / *Hirpida* + *Hirpsinjaevia* with either Hemileucinae + Ceratocampinae + Arsenurinae or Saturniinae + Salassinae. In panel (b), average values of GC content and saturation (R-squared of the regression between pairwise distances calculated from aligned sequences and branch length) for loci that significantly supported topologies *A*/*Abis* (i.e., Pvalue of the AU test ≦ 0.05; N loci = 189; Table S3) or not (Nloci=796) were compared using a randomization test (N randomization = 9999; c2m function of the R package *rich*) and P values are reported on graph.

Analysis of Conflicting Topologies

A single important conflict was observed among the trees with respect to the position of Agliinae and of species in the *Hirpida* + *Hirpsinjaevia* clade (Figs. 1 and S1): (1) Agliinae and *Hirpida* + *Hirpsinjaevia* either formed a clade sister to Arsenurinae + Ceratocampinae + other Hemileucinae (ACH) (IQ-TREE; topology A), or branched sequentially with Agliinae sister to a clade grouping *Hirpida* + *Hirpsinjaevia* and ACH (ASTRAL90; topology Abis); or (2) *Hirpida* + *Hirpsinjaevia* grouped with ACH while Agliinae grouped with Salassinae + Saturniinae (ASTRAL70; topology B); or (3) Agliinae and *Hirpida* + *Hirpsinjaevia* formed a grade basal to Salassinae + Saturniinae (ASTRAL50; topology C). The contrasting results obtained with ASTRAL and the gCFs of the Agliinae + *Hirpida* + *Hirpsinjaevia* clade in the IQ-TREE trees (8.6%; Fig. S1) highlight conflict among gene trees. GGI analyses show that of the 985 UCEs available for both Agliinae and *Hirpida* + *Hirpsinjaevia* species, 540 (54.8%) favored topologies A/Abis; 228 (23.2%) favored topology B; and 217 (22.0%) favored topology C (Table S3). In addition, topologies A/Abis were a significantly better explanation for 189 (19.2%) of the gene trees while topology B was a significantly better explanation for only 3 (0.3%) of the gene trees, and topology C was a significantly better explanation for 9 (0.9%) of the gene trees. Statistical analyses of UCE properties show that topologies A/Abis were supported by UCEs with lower saturation (Fig. 1(2)). Further

analyses of data subsets comprising the 20% least saturated (*n*=204) or 50% most saturated (*n*=512) loci confirmed that the placement of Agliinae as sister to Salassinae + Saturniinae was likely an artefact caused by saturation of phylogenetic signal (Fig. S2). Both IQ-TREE and ASTRAL90 analyses of the least saturated UCEs recovered Agliinae close to ACH (topologies A/Abis; Fig. 1a), while Agliinae always jumped into the Saturniinae + Salassinae part of the tree when analysis focused on the most saturated loci (Fig. S2). In addition, taxon-based analysis of systematic bias did not reveal evidence that the sister taxa relationship between Agliinae and *Hirpida* + *Hirpsinjaevia* (topologies A/Abis; Fig. 1a) resulted from compositional (GC) bias or LBA (Fig. S3).

Finally, regardless of the conflicting placement of the subfamily Agliinae, IQ-TREE and ASTRAL analyses based on the least saturated half of the loci produced the most similar topologies (RF distances; Table S3). Consequently, subsequent analyses focused on the phylogram derived from the IQ-TREE analyses of the 50% least saturated UCEs (*n*=512; Figs. 2 and S2I).

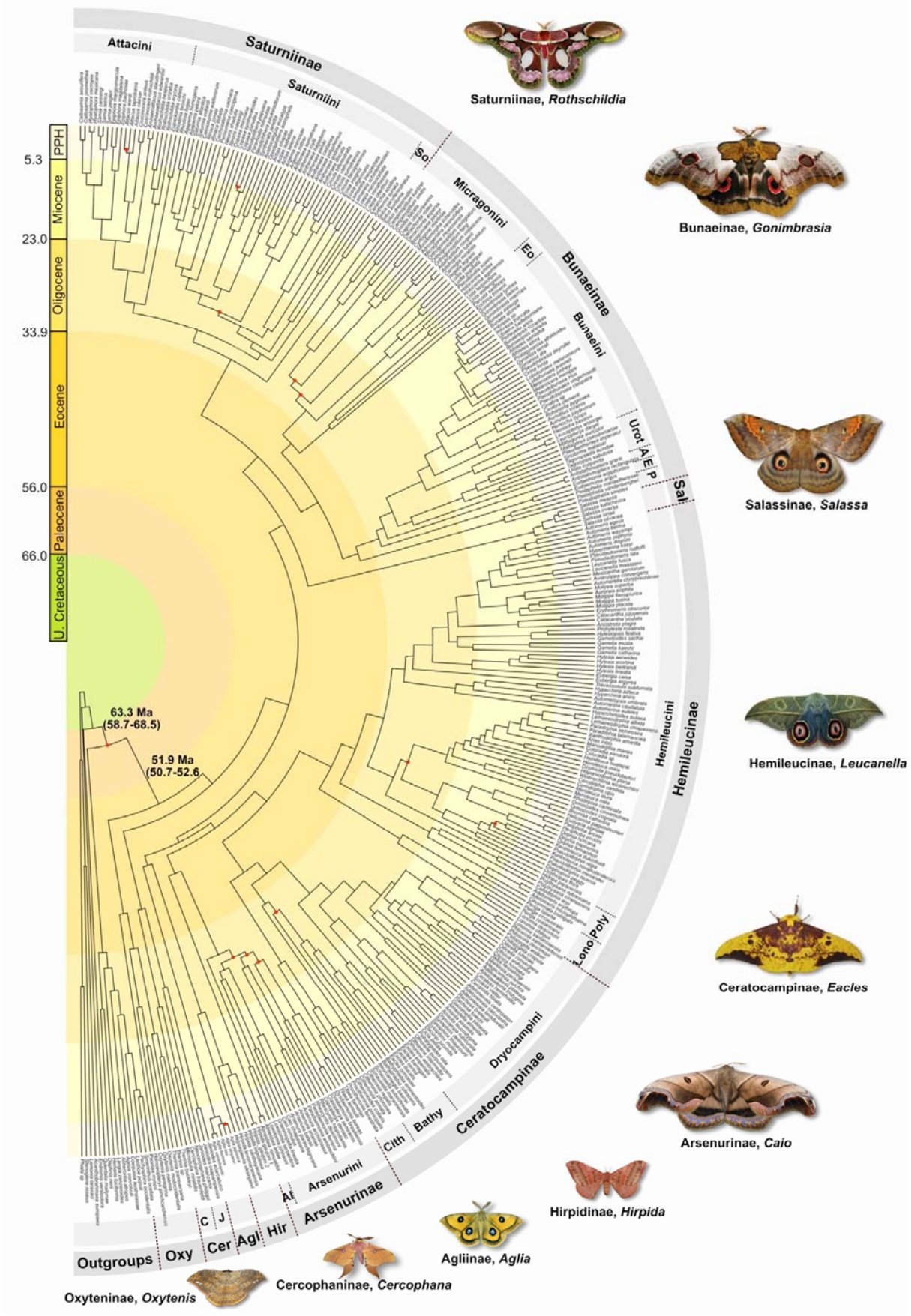

Figure 2. Saturniidae tree of life. The classification proposed in this study is displayed on the chronogram (MCMCtree, uncorrelated relaxed clock model) inferred from the topology selected after exploration of systematic bias (i.e., the IQ-TREE tree inferred from the 50% least saturated loci). Red dots at nodes identify poorly supported nodes (SHaLRT<80 or UFBoot<95). Abbreviations used: A = Antistathmopterini; Agl = Agliinae; Al = Almeidaiini; Bathy = Bathyphlebiini; C = Cercophanini; Cer = Cercophaninae; Cith = Citheroniini; E = Eudaemoniini; Eo = Eochroini; Hir = Hirpidinae; J = Janiodini; Lono = Lonomiini; Oxyteninae; P = Pseudapheliini; Poly = Polythysanini; Sal = Salassinae; So = Solini; Urot = Urotini.

Divergence Time Estimates and Historical Biogeography

Analyses based on both autocorrelated and uncorrelated relaxed clock models provided similar results (median of differences between mean or median ages of all nodes = 1.65 Myr; Table S4), therefore we only represent (Figs. 2 and 3) and cite estimates based on the uncorrelated relaxed clock model in main text for brevity. The divergence times and confidence intervals for correlated and uncorrelated clock models are provided in Table S4 for all nodes (see also Figure S4 for the chronograms), while those of clades discussed below are provided in Table 1.

	Stem (in Myr)		**Crown (in Myr)**	
Clades	**Uncorrelated**	**Correlated**	**Uncorrelated**	**Correlated**
ACH	45.11 [42.93-47.18]	42.94 [39.69-45.31]	44.08 [41.85-46.19]	42.05 [38.85-44.51]
Agapema	11.90 [9.76-14]	14.02 [11.89-16.60]	4.85 [2.81-7.06]	5.78 [3.7-7.94]
Agliinae	42.95 [39.88-45.81]	41.44 [38.10-44.26]	3.09 [2.20-4.06]	13.01 [8.94-16.40]
Agliinae + Hirpidinae + ACH	45.98 [43.88-47.97]	43.65 [40.50-45.94]	45.11 [42.93-47.18]	42.94 [39.69-45.31]
American *Antheraea* (*Telea*)	8.36 [5.95-10.91]	9.51 [7.10-11.77]	3.93 [2.34-5.67]	4.67 [3.16-6.30]
Antherina + *Ceranchia*	27.20 [24.78-29.65]	28.34 [25.43-31.24]	7.61 [4.42-11.23]	11.05 [7.21-14.94]
Argema	14.53 [12.12-17.01]	13.30 [10.63-15.68]	10.63 [8.03-13.22]	9.81 [7.54-12.05]
Arsenurinae	44.08 [41.85-46.19]	42.05 [38.85-44.51]	40.04 [36.06-43.62]	39.52 [36.06-42.25]
BSS	45.98 [43.88-47.97]	43.65 [40.50-45.94]	43.36 [40.97-45.65]	41.46 [38.34-43.87]
Bunaea (Madagascar colonization)	[-]	[-]	2.00 [1.21-2.87]	1.91 [1.32-2.53]
Bunaeinae	40.17 [37.61-42.67]	38.27 [35.48-40.87]	37.22 [34.66-39.78]	35.24 [32.48-37.74]
Calosaturnia	14.16 [12.01-16.12]	16.58 [14.42-19.38]	[-]	[-]

Ceratocampinae	41.84 [39.51-44.07]	39.33 [36.32-41.92]	35.97 [33.04-38.83]	32.02 [28.43-35.05]
Ceratocampinae + Hemileucinae	44.08 [41.85-46.19]	42.05 [38.85-44.51]	41.84 [39.51-44.07]	39.33 [36.32-41.92]
Cercophaninae	49.61 [47.96-51.04]	48.92 [46.36-50.67]	38.08 [31.29-43.79]	39.99 [34.91-44.22]
Copaxa	21.11 [18.71-23.48]	22.37 [19.87-25.02]	10.89 [7.96-14.03]	9.92 [6.94-13.03]
Coscinocera	11.21 [8.61-13.93]	11.28 [8.75-14.14]	2.04 [1.15-3.06]	1.87 [1.03-2.81]
Eosia	17.02 [13.86-20.19]	15.98 [13.05-19.48]	4.18 [2.49-6.05]	2.76 [1.50-4.19]
Epiphora	14.51 [12.18-17.06]	14.60 [11.88-17.77]	6.62 [4.64-8.73]	5.91 [3.86-8.13]
Eupackardia + *Rothschildia*	21.72 [18.92-24.58]	22.20 [19.05-25.43]	10.83 [8.12-13.71]	11.65 [8.48-14.97]
Hemileucinae	41.84 [39.51-44.07]	39.33 [36.32-41.92]	36.48 [33.72-39.27]	32.17 [29.08-35.06]
Hirpidinae	42.95 [39.88-45.81]	41.44 [38.10-44.26]	19.03 [13.31-25.18]	23.87 [17.69-29.91]
Maltagorea	11.56 [9.09-14.00]	8.78 [6.46-11.13]	8.34 [5.94-10.82]	6.63 [4.69-8.58]
Opodiphthera clade	20.92 [18.65-23.28]	21.77 [19.27-24.38]	11.80 [9.46-14.25]	11.60 [8.80-14.47]
Oxyteninae	51.90 [50.66-52.55]	51.52 [49.25-52.55]	37.10 [31.08-43.13]	31.63 [24.19-38.56]
Saturniidae	63.27 [58.69-68.51]	63.96 [59.74-68.52]	51.90 [50.66-52.55]	51.52 [49.25-52.55]
Sinobirma	14.02 [11.46-16.53]	10.56 [7.91-13.16]	[-]	[-]

Table 1. Summary of mean divergence time estimates and 95% highest posterior density (HPD) for groups or colonization events discussed. Mean and median ages with 95% HPD for all nodes are provided in Table S4. Units are in Myr. Our new classification is used for taxon names. ACH = Arsenurinae + Ceratocampinae + Hemileucinae; BSS = Bunaeinae + Salassinae + Saturniinae.

The stem age of Saturniidae was estimated in the early Cenozoic at about 63 Ma. The Oxyteninae and Cercophaninae originated about 52 Ma and 50 Ma, respectively. All other subfamilies originated during a brief interval (4 Myr) in the middle Eocene (46-42 Ma) and diversified during the Oligocene and Miocene. While only 32 (18%) of the 180 extant genera had appeared before the end of the Oligocene (including all 9 genera of Arsenurini), the remaining bulk of extant saturniid genera originated during the Miocene (Fig. 3).

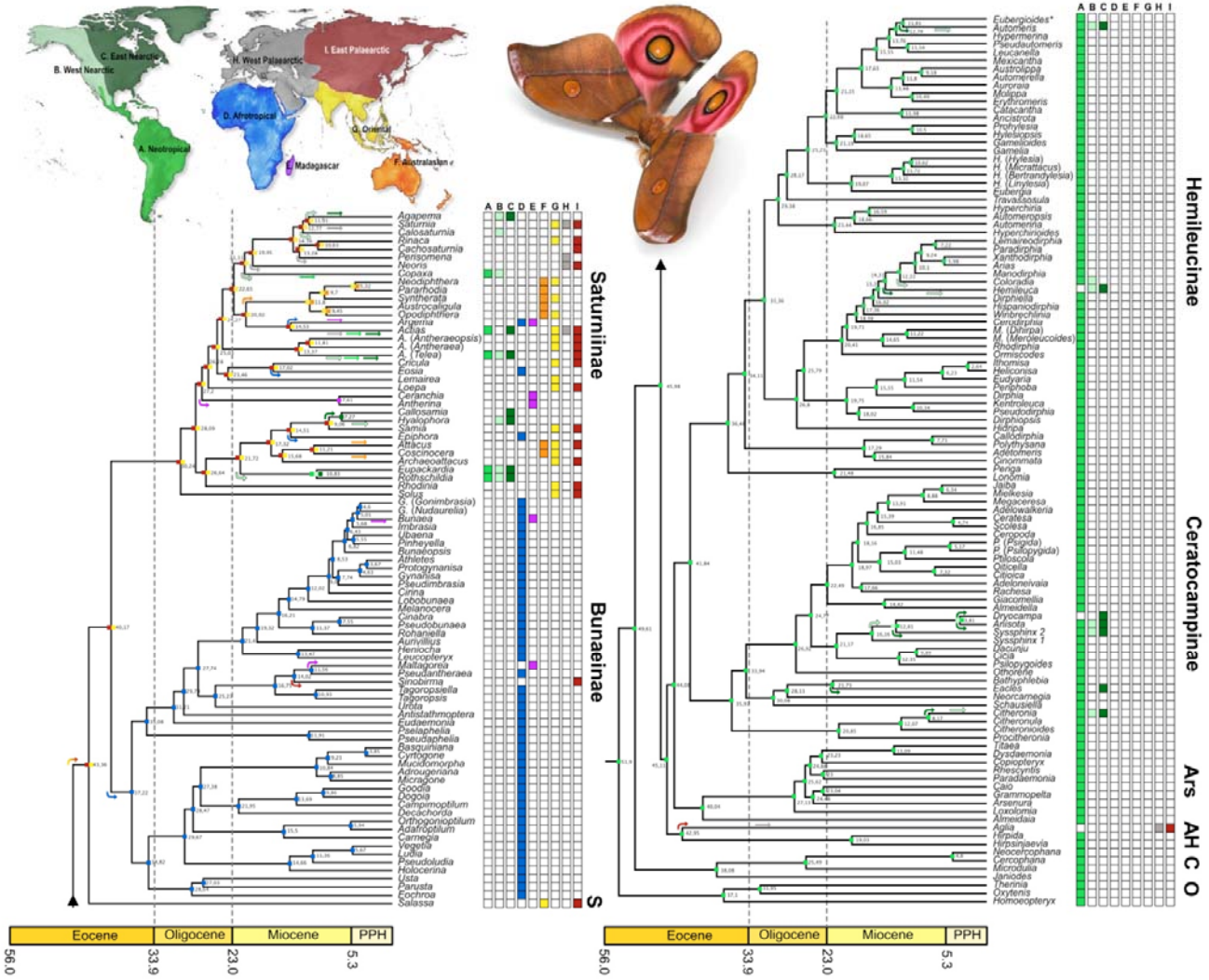

Figure 3. Global historical biogeography of Saturniidae. Ancestral ranges were inferred with the BAYAREALIKE+J model (best-fit and most plausible model according to empirical considerations; see text) as implemented in *BioGeoBEARS*. Alternative inferences of ancestral ranges are provided in Figure S5. The chronogram is derived from the species-level chronogram obtained with the uncorrelated relaxed clock model implemented in MCMCtree (see Fig. 2) that was pruned to keep only one specimen per genus/subgenus. The classification proposed in this study is used to annotate the tree. Colored boxes following each terminal name represent biogeographical regions A to I as illustrated in the upper-left map; colored arrows refer to inferred dispersal/colonization events. Abbreviations used: A = Agliinae; Ars = Arsenurinae; C=Cercophaninae; H = Hirpidinae; O = Oxyteninae; S = Salassinae. PPH=Pliocene, Pleistocene and Holocene. Illustrative photograph = *Antherina suraka* (Saturniinae); image courtesy of Armin Dett.

With respect to historical biogeography, inclusion of the parameter *J* (jump dispersal events during cladogenesis) in models of geographic range evolution remains controversial, as is the validity of statistical comparisons of models with and without *J* (Ree and Sanmartín 2018; Matzke 2021). Empirical considerations have been advocated as an alternative way to select among biogeographical scenarios (Ree and Sanmartin 2018). Here, both AICc and the observation that most extant subfamilies occupy a single biogeographical area favor biogeographical models that include the *J* parameter (Table S2, Fig. S5). Without it, the DEC model had the best fit, but inferred a widespread ancestor for the family with multiple subsequent local extinctions. When the *J* parameter was included, BAYAREALIKE+J was inferred as the best-fit model (Table S2) and all ancestral range estimations unambiguously supported a Neotropical origin for saturniids.

Given the most likely ancestral areas estimation, saturniid biology, and palaeogeological knowledge, following their origin in the Neotropics, the Saturniidae likely colonized the Old World twice during the mid-Eocene, probably through Beringia. These two

412 dispersal events involved an ancestor of Salassinae + Saturniinae between 46 and 43 Ma, and
413 an ancestor of Agliinae at 43 Ma (red arrows in Figure 3). Shortly later, a lineage (represented
414 by three tribes - Bunaeini, Micragonini and Urotini - in the current classification) colonized
415 Africa between 40 and 37 Ma and subsequently diversified extensively (with 55 extant
416 genera). This lineage remained restricted to this continent except for three lineages which
417 dispersed to new areas: *Sinobirma* invaded the Oriental region (*ca*. 14 Ma), while *Maltagorea*
418 (*ca*. 12 Ma) and *Bunaea* (*ca*. 2 Ma) colonized Madagascar. By contrast, the Attacini and
419 Saturniini tribes in Saturniinae not only diversified in the Oriental and East Palearctic regions,
420 but also dispersed multiple times from there to adjacent areas (Fig. 3). They colonized Africa
421 and Madagascar on four occasions during the mid-Miocene Climatic Optimum (*Epiphora* 14
422 Ma, *Argema* 14 Ma, *Eosia* 17 Ma, and the clade *Antherina* + *Ceranchia* 27 Ma). They also
423 dispersed through Sunda and Wallacea on multiple times, crossing Lydekker's line on three
424 occasions (*Attacus*, *Coscinocera*, *Austrocaligula* clade). Finally, they returned seven times to
425 the New World with two relatively ancient dispersal events (early Miocene; *Copaxa* 21 Ma
426 and the clade *Eupackardia* + *Rothschildia* 21 Ma) and five others during the second half of
427 Miocene (*Actias* 14 Ma, *Antheraea* (*Telea*) 13 Ma, *Calosaturnia* 13 Ma, *Agapema* 12 Ma, and
428 the clade *Hyalophora* + *Callosamia* 7 Ma). The diverse Neotropical fauna of saturniids
429 colonized the Nearctic region only seven times (Fig. 3, right-hand section of tree, green
430 arrows) and all these dispersal events postdated the final formation of the Isthmus of Panama
431 (*ca*. 15 Ma).
432

433 **DISCUSSION**

434 *A Comprehensive Genus-level Phylogeny of Saturniidae*

435

436 This study expands upon earlier investigations (Regier et al. 2008, Barber et al. 2015,
437 Hamilton et al. 2019) to yield a comprehensive and robust phylogenetic framework for higher
438 relationships within Saturniidae. The results confirm that Oxyteninae and Cercophaninae
439 were the first two subfamilies to diverge and that Salassinae is sister to Saturniinae. The
440 present results agree with those of Barber et al. (2015) and Hamilton et al. (2019) as they
441 place Arsenurinae as sister to Ceratocampinae + Hemileucinae (but without *Hirpida* +
442 *Hirpsinjaevia*; see below). However, in-depth analysis of conflict among gene trees shows
443 that subfamily Agliinae, whose position remained unelucidated, belongs to a lineage that also
444 includes the new-world subfamilies Arsenurinae, Ceratocampinae, and Hemileucinae. This
445 suggests that its alternative placement as sister to Salassinae and Saturniinae as obtained by
446 Hamilton et al. (2019) was also likely an artefact of tree reconstruction, possibly caused by
447 the saturation of nucleotide sequences. Indeed, when these authors analyzed the AHE loci
448 using protein sequence data which saturate less rapidly owing to a larger state space (20
449 possible amino acids; see their additional file 8), they recovered Agliinae as more closely
450 related to new-world subfamilies. These relationships are corroborated by larval characters
451 shared with Arsenurinae (Michener 1952; e.g., D2 setae on abdominal segment A9 of first
452 instar larva form a median scolus or chalaza; first larval stages bear two or more pairs of large
453 thoracic horns forked at their apices). Interestingly, our analyses are the first to examine the
454 genera *Hirpida* and *Hirpsinjaevia* and they reveal that these two closely related Neotropical
455 genera are sister to Agliinae. Unfortunately, the host plant(s) and immature stages of *Hirpida*
456 and *Hirpsinjaevia* are unknown but, based on their phylogenetic placement, we predict that
457 their first instar larvae bear large thoracic horns and may feed on Fagaceae and/or Betulaceae
458 like the Agliinae.

459 In the arsenurine tribe Arsenurini, Hamilton et al. (2021) found from a thorough
460 phylogenomic analysis of hundreds of AHE genes that phylogenetic signal remained elusive,

likely reflecting a burst of diversification. Our analysis also found that relationships among its component genera are poorly supported (Figs. 2 and S2I) and are discordant from the hypothesis preferred by Hamilton et al. (2021). This casts doubt on current understanding of their evolutionary history, an uncertainty that can only be resolved by further investigation, perhaps by combining AHE and UCE loci and expanding taxon sampling. Within the Ceratocampinae and Hemileucinae, our results provide the first robust, comprehensive hypothesis of relationships among its genera. They fully agree with conclusions based on a 6-gene data set and limited taxon sampling (Barber et al 2015), but largely contradict groupings proposed for Ceratocampinae by Balcazar-Lara & Wolfe (1997) based on their cladistic analysis of both adult and immature morphology.

Within Saturniinae, our results unequivocally support the position of *Rhodinia* as sister to members of the Attacini, in agreement with AHE-based conclusions (Rubin et al. 2018) and recent findings from the analysis of mitogenomes (Chen et al. 2021). In addition, as our sampling examined all genera in the tribe Urotini – considered to represent an artificial grouping of several unrelated lineages (Oberprieler 1997; Rougerie 2005; Barber et al 2015; Rubin et al 2018) – the outcome of our analyses offers the first robust framework of the evolutionary history of African saturniids to lay down a new classification.

Taxonomic Implications

Our phylogenetic hypothesis has important and unexpected implications for the classification of Saturniidae (Fig. 2). We propose several taxonomic changes that are detailed below and summarized as a complete genus-level checklist (SI Appendix S1; see also Table S1). The unexpected placement of *Hirpida* + *Hirpsinjaevia* as sister to Agliinae as well as the age of the lineage justify the erection of a new subfamily: Hirpidinae Rougerie **subfam. nov**. As all three previously recognized Afrotropical tribes of Saturniinae (Bunaeini, Urotini,

Micragonini) form a monophyletic group sister to all other Saturniinae (Attacini, Saturniini and Solus), we adopt here the classification proposed by Nässig et al. (2015) that recognizes this clade as subfamily Bunaeinae Bouvier, **1927 stat. rev.**. Within this subfamily, we consider Bunaeini, Micragonini, and Urotini as monophyletic tribes but with new circumscriptions ensuring their monophyly. To achieve this, we describe a new tribe and resurrect three others involving the following seven genera: *Eochroa* (previously in Bunaeini), *Parusta* and *Usta* are assigned to Eochroini Cooper, 2002 **stat. rev.**; *Pseudaphelia* and *Pselaphelia* to Pseudapheliini Packard, 1914 **stat. rev.**; *Eudaemonia* to Eudaemoniini Packard, 1902 **stat. rev.**; and *Antistathmoptera* to Antistathmopterini Rougerie **trib. nov.**. The rare, enigmatic east African genus *Eosia* Le Cerf,1911 (Bouyer 2002), previously placed within Micragonini (Bunaeinae), is recovered as sister to *Cricula* Walker, 1855 of the Saturniini (Saturniinae) to which it is transferred, a position which agrees with evidence from the morphology of first instar larva (Rougerie 2005). The genus *Solus*, whose phylogenetic placement is clarified here for the first time, is sister to Attacini + Saturniini, a position that requires the erection of a new tribe: Solini Rougerie **trib. nov.**. We also propose to follow Nässig (1991) in considering *Graellsia* Grote, 1896 to be a junior synonym of *Actias* Leach, 1815. Since our results propose the first robust, comprehensive phylogeny for the two most diverse subfamilies of new-world Saturniidae, we propose a new tribal arrangement for their genera (Fig. 2; see Table S1 and Appendix S1 for details): (1) in Ceratocampinae, we resurrect the following three tribes: Bathyphlebiini Travassos & Noronha, 1967 **stat. rev.**, Ceratocampini Harris, 1841 **stat. rev.**, and Dryocampini Grote & Robinson, 1866 **stat. rev.**; and (2) in Hemileucinae, we expand the previously monotypic tribe Polythysanini Michener 1952 by adding the genera *Adetomeris*, *Callodirphia*, and *Cinommata*; resurrect tribe Lonomiini Bouvier, 1930 **stat. rev.** for genera *Lonomia* and *Periga*; and exclude *Catharisa cerina* Jordan 1911, considered until now as an hemileucine (Lemaire 2002, Smith et al.

2013), while we recovered it nested within the genus *Eacles* of the Ceratocampinae. This unexpected placement agrees with recent observations of the morphology of its first instar caterpillars (P. Smith, pers. comm.) and leads us to treat *Catharisa* Jordan, 1911 **syn. nov.** as a junior synonym of *Eacles* Hübner, [1819], with *Eacles cerina* **comb. nov.** transferred within Bathyphlebiini of the Ceratocampinae. Within the Hemileucinae, the monotypic genus *Eubergioides* Michener, 1949 **syn. nov.** appears nested within *Automeris* Hübner, [1819], an affinity already suggested by Michener (1952) based on the comparison of male genitalia; it is considered a junior synonym of the latter, with *Automeris bertha* (Schaus, 1896) **comb. nov.** transferred to genus *Automeris*. Among the African bunaeine saturniids, we resurrect the genus *Pinheyella* Cooper, 2002 **stat. rev.** for *P. anna* Maassen, 1985 **comb. nov.** whose current placement in genus *Gonimbrasia* Butler, 1878 makes that genus polyphyletic. Finally, we note that our results question the monophyly of six genera, but we refrain from proposing nomenclatural change as limited sampling within each genus impedes proper circumscription of natural groups: *Neodiphthera* Fletcher, 1982; *Ludia* Wallengren, 1865; *Molippa* Walker, 1855; *Pseudodirphia* Bouvier, 1928; *Kentroleuca* Draudt, 1929; and *Syssphinx* Hübner, [1819]. From here on, subfamily, tribe and genus names refer to the new classification proposed in this study (Fig. 2; Appendix S1).

Historical Biogeography

This work represents a first investigation of the historical biogeography of saturniids (Fig. 3) based on a robust dated phylogeny that includes all known extant genera. It reveals that the family originated in the Neotropics shortly after the Cretaceous-Paleogene boundary. Its diversification was marked by a key split about 46 Ma between lineages AACHH (formed by subfamilies Agliinae, Arsenurinae, Ceratocampinae, Hemileucinae and Hirpidinae; >2,000 extant species in 96 genera) and BSS (Bunaeinae, Salassinae and Saturniinae; >1,350 species

in 86 genera). The former remained confined to the New World except for the Agliinae (see below), while the later diversified in all biogeographical regions, before recolonizing the New World on several occasions. This split had been preceded by two earlier branching lineages (first Oxyteninae 52 Ma, then Cercophaninae 50 Ma) that have remained restricted to South America where they comprise 70 and 122 extant species respectively (Kitching et al. 2018, Brechlin 2020).

Dispersal out of the Neotropics and into the Old World of the ancestors of lineage BSS occurred during the middle Eocene (46-43 Ma). As dispersal across the oceanic barriers separating the New and Old Worlds seems unlikely, it is more likely that dispersal occurred via the Nearctic during the mid-Eocene Climatic Optimum, a transient period of global warming (Westerhold et al. 2020). This would have required over-water dispersal through an archipelago in the Panamanian gap (Pindell et al. 2005, Iturralde-Vinent 2006) or via the Caribbean Arc that subsided toward the end of the Eocene (Pindell et al. 2005, Philippon et al. 2020, Cornée et al. 2021, Garrocq et al. 2021) before their northward dispersal. At this time period, further dispersal of the BSS ancestors from the Nearctic into the Eastern Palearctic, and from there southwards into the Oriental region would have been possible through the Boreotropical forest belt (Morley 2003, 2011), which extended as far as the Arctic Circle, facilitating faunal exchanges (Jahren 2007). Our results also suggest that ancestors of the Agliinae, within the AACHH lineage, likely used the same route through Beringia about 43 Ma as an independent long-distance dispersal from the New to Old World. Interestingly, the food plants (Ballesteros-Mejia et al 2020) of both Agliinae and early lineages of the BSS lineage (e.g., beech, oak, maple, plum trees, sumac) were well represented in the forests of the northern hemisphere during middle Eocene (Jahren, 2007), thus lending support to this dispersal route.

560 During this same period (Fig. 3; 40-37 Ma), ancestors of Bunaeinae dispersed from the
561 Oriental to African region. This dispersal was facilitated by the mixed deciduous and
562 evergreen forests occurring in Central Asia and by the presence of archipelagoes and land
563 connections. Between 41 and 35 Ma, Balkanotolia, an archipelago that spanned the
564 Neotethyan margin (Licht et al., 2022) and the Alboran/Apulian platforms
565 emerged (Vandenberghe et al. 2012), possibly facilitating the colonization of Africa. This
566 dispersal may have been driven by the climatic deterioration (or "Grande Coupure")
567 (Hartenberger 1998, Licht et al. 2022) that occurred during the Eocene-Oligocene transition
568 period, effectively forcing the Bunaeinae ancestor to seek warmer conditions southward.
569 Interestingly, several groups of mammals (e.g., rodents, primates) with excellent fossil
570 records also colonized Africa near the Bartonian-Priabonian boundary (*ca* 37.8 Ma) (Huchon
571 et al. 2007, Chaimanee et al. 2012, Marivaux et al. 2014, Coster et al. 2015, Licht et al. 2022).
572 After colonizing Africa, the ancestral Bunaeinae experienced a spectacular diversification as
573 all extant tribes had appeared by the early Oligocene. Further investigation of the importance
574 of different key innovations (ecological or morphological) that have triggered this
575 diversification burst constitute an interesting perspective.
576 As cooling during the Eocene–Oligocene disrupted the belt of Boreotropical forests, the
577 accretion of ice sheets broke the Beringian connection, leading to the divergence of ancestral
578 Saturniinae in these forests. Our analyses (Figs. 3 and S5) show that the Saturniinae and most
579 of its lineages originated in the Oriental + Eastern Palearctic region, but as the Boreotropical
580 forests contracted drastically during the "Grande Coupure", this likely forced southward
581 displacements of their ranges into refuges in the Sino-Himalayan mountains of the Eastern
582 Palearctic region (LePage et al. 2005, Xing and Ree 2017, Jia and Bartish 2018). The
583 observation that the diversity of non-African members of the BSS clade peaks in the Sino-
584 Himalayan mountains may reflect the role of this transition zone as a hub for further

585 diversification of these moths. A number of Saturniinae lineages subsequently dispersed and
586 diversified extensively in the Oriental and Palearctic regions, colonizing the Western
587 Palearctic four times: *Neoris* (stem age 20 Ma), *Perisomena* (13 Ma), *Saturnia* (12Ma), and
588 *Actias* (7 Ma). They also colonized Australasia (the *Opodiphthera* group (21 Ma) and
589 *Coscinocera* (11 Ma) within the Attacini), the Afrotropics (*Epiphora* (14 Ma), *Eosia* (17 Ma)
590 and *Argema* (14 Ma)), and the Nearctic and Neotropical regions (*Eupackardia* + *Rothschildia*
591 (22 Ma), *Copaxa* (21 Ma), *Calosaturnia* (13 Ma), and *Agapema* (12 Ma)). Interestingly, a
592 single dispersal event by a member of the genus *Sinobirma* (subfamily Bunaeinae) occurred
593 from Africa to the Eastern Palearctic region, nearly synchronous (14 Ma) with the
594 colonization of the Afrotropics by *Epiphora*, *Eosia*, and *Argema.* These range expansions
595 may have been facilitated by the collision of the Arabian plate with Eurasia *ca.* 15 Ma (Rogl
596 1999, Harzhauser et al. 2007).
597
598 *Final Remarks*
599 Our knowledge of insect evolution remains strongly impeded by both the scale of their
600 diversity and the difficulty to generate accurate and robust spatial and evolutionary
601 frameworks based on comprehensive coverage. Currently, only a few densely sampled and
602 time-calibrated phylogenies have been generated in diverse groups of insects, bringing
603 insights into the origins of observed diversity patterns such as the latitudinal diversity gradient
604 (e.g., Condamine et al. 2012, Chazot et al. 2021 for butterflies; Economo et al. 2018 for ants),
605 or the influence of life-history traits on diversification dynamics (Sota et al. 2022). We
606 believe that the Saturniidae family, as one of the best-documented family of insects with
607 global distribution and high species-richness, represents a new promising model to further
608 investigate the mechanisms driving diversification in insects. Our results have revealed that
609 the spatial dynamism of Saturniinae (33 genera, 741 species) is in striking contrast (Fig. 3) to

610 the situation in other subfamilies that also diversified extensively (Bunaeinae: 50 genera, 580
611 species; Ceratocampinae: 30 genera, ca. 300 species; Hemileucinae: 55 genera, ca. 1600
612 species; see Kitching et al. (2018)), but remained restricted to the biogeographical region
613 where they originated: Bunaeinae in the Afrotropical region (except for *Sinobirma*, and
614 including two independent colonization of Madagascar); Ceratocampinae and Hemileucinae
615 in the Neotropics with limited dispersal to the Nearctic region. The reasons for these
616 contrasting dispersal patterns remain unclear, but differing life-history traits, such as larval
617 diet and pupation modes (cocoons in Saturniinae are among the strongest within the family)
618 may have facilitated long-distance dispersal and range expansion. In general, the new spatial
619 and temporal framework produced here for the evolution of wild silkmoths opens new
620 avenues of research to understand the intriguing success of these capital-breeding moths that
621 managed to occupy all biogeographical regions today and to represent one of the most diverse
622 and abundant group of large-sized insects.
623
624 **FUNDING**
625 This work was supported by French National Research Agency (SPHINX: ANR-16-
626 CE02-0011-01, GAARAnti: ANR-17-CE31-0009, LABEX CEBA: ANR-10-LABX-25-01
627 and LABEX TULIP: ANR-10-LABX-41); French Foundation for Research on Biodiversity
628 (FRB) and Centre for the Synthesis and Analysis of Biodiversity (CESAB: ACTIAS grant).
629
630 **ACKNOWLEDGEMENTS**
631 We are thankful to the Canadian Centre for DNA Barcoding and Centre for Biodiversity
632 Genomics at University of Guelph (Ontario, Canada) as well as to all the participants to the
633 Saturniidae DNA barcoding campaign for their contributions to the assembly of samples. We
634 thank Corinne Poitout, Hélène Vignes and Audrey Weber (INRAE and CIRAD, AGAP,

France) for their assistance to sequencing, and the Genotoul bioinformatics platform (Toulouse, Occitanie, France) for providing computing resources.

TAXONOMIC APPENDIX – NEW HIGHER TAXA

Hirpidinae Rougerie, **subfamilia nova**

http://zoobank.org/LSID######

Type genus: *Hirpida* Draudt, 1930

This subfamily comprises two Andean genera, *Hirpida* and *Hirpsinjaevia*. A suggested combination of diagnostic features includes the following characters of the adults proposed by Michener (1952) as distinctive for genus *Hirpida*: head with the sides of the frons slightly convex; tarsomeres with spines on their ventral surface; well-developed arolia and pulvilli; absence or reduction of vein 3A in hindwings; tegulae long, reaching the anterior median angle of mesothoracic scutellum; anepisternal suture largely horizontal but directed slightly downward posteriorly; male genitalia with free juxta and articulated valvae. The status of these characters remains unknown in the recently described, rare genus *Hirpsinjaevia* as it could not be examined for this study. Further comparative morphology and a formal phylogenetic analysis of characters are needed to identify unique characters or more likely a unique combination of characters that can accurately diagnose members of the subfamily Hirpidinae.

Antistathmopterini Rougerie, **tribus nova**

http://zoobank.org/LSID######

Type genus: *Antistathmoptera* Tams, 1935

This tribe only includes species in the genus *Antistathmoptera*, all of which appear restricted to Eastern Africa. Because of their rarity in collections, little is known of their

morphology, but they can be easily distinguished by a unique combination of adult characters: long tailed hindwings; pointed forewing apex; both pairs of wings with a discal spot formed of two contiguous hyaline areas.

Solini Rougerie, **tribus nova**

http://zoobank.org/LSID######

Type genus: *Solus* Watson, 1913

This tribe only includes the genus *Solus* which is restricted to the continental part of the Oriental region. The following combination of characters in adults are diagnostic: vein d3 of forewing discal cell missing, resulting in an open discal cell; lower branch of fork at the start of forewing vein 1A+2A much thinner than the upper branch; extremity of axillary sclerite 1 of forewings rounded; anapleural suture of mesothorax reduced; galeae present, short and broad.

LITERATURE CITED

Arcila D., Orti G., Vari R., Armbruster J.W., Stiassny M.L.J., Ko K.D., Sabaj M.H., Lundberg J., Revell L.J., Betancur-R R. 2017. Genome-wide interrogation advances resolution of recalcitrant groups in the tree of life. Nat. Ecol. Evol. 1: 0020.

Balcazar-Lara M., Wolfe K.L. 1997. Cladistics of the Ceratocampinae (Lepidoptera: Saturniidae). Trop. Lepid. Res. 8: 1-53.

Barber J.R., Leavell B.C., Keener A.L., Breinholt J.W., Chadwell B.A., McClure C.J.W., Hill G.M., Kawahara A.Y. 2015. Moth tails divert bat attack: evolution of acoustic deflection. PNAS. 112: 2812-2816.

Battisti A., Holm G., Fagrell B., Larsson S. 2011. Urticating hairs in arthropods: their nature and medical significance. Annu. Rev. Entomol. 56: 203-220.

Bergsten J. 2005. A review of long-branch attraction. Cladistics. 21:163-193.

Betancur-R R., Arcila D., Vari R.P., Hughes L.C., Oliveira C., Sabaj M.H., Orti G. 2019. Phylogenomic incongruence, hypothesis testing, and taxonomic sampling: the monophyly of characiform fishes. Evolution. 73: 329-345.

Borowiec M. 2019. Convergent evolution of the army ant syndrome and congruence in big-data phylogenetics. Syst. Biol. 68: 642-656.

Borowiec M., Rabeling C., Brady S., Fisher B., Schultz T., Ward P. 2019. Compositional heterogeneity and outgroup choice influence the internal phylogeny of the ants. Mol. Phylogenet. Evol. 134: 111-121.

Borowiec M.L. 2016. AMAS: a fast tool for alignment manipulation and computing of summary statistics. PeerJ. 4: e1660.

Borowiec M.L., Lee E.K., Chiu J.C., Plachetzki D.C. 2015. Extracting phylogenetic signal and accounting for bias in whole-genome data sets supports the Ctenophora as sister to remaining Metazoa. BMC genomics. 16:987.

699 Bossert S., Murray E.A., Blaimer B.B., Danforth B.N. 2017. The impact of GC bias on
700 phylogenetic accuracy using targeted enrichment phylogenomic data. Mol. Phylogenet.
701 Evol. 111: 149-157.
702 Bouckaert R., Vaughan T., Barido-Sottani J., Duchêne S., Fourment M., Gavryushkina A.,
703 Heled J., Jones G., Kühnert D., De Maio N., Matschiner M., Mendes F.K., Müller N.F.,
704 Ogilvie H.A., du Plessis L., Popinga A., Rambaut A., Rasmussen D., Siveroni I., Suchar
705 M.A., Wu C.-H., Xie D., Zhang C., Stadler T., Drummond A.J. 2019. BEAST 2.5: An
706 advanced software platform for Bayesian evolutionary analysis. PLoS Comput. Biol.
707 15: e1006650.
708 Boussau B., Walton Z., Delgado J.A., Collantes F., Beani L., Stewart I.J., Cameron S.A.,
709 Whitfield J.B., Johnston J.S., Holland P.W.H., Bachtrog D., Kathirithamby J.,
710 Huelsenbeck J.P. 2014. Strepsiptera, phylogenomics and the Long Branch Attraction
711 problem. Plos One. 9: e107709.
712 Bouyer T. 2002. Description du mâle supposé d'*Eosia insignis* Le Cerf, 1911 (Lepidoptera
713 Saturniidae). Entomologia Africana. 7: 3-14.
714 Brechlin R 2020. A revision of the genus *Janiodes* Jordan, 1924 (Lepidoptera: Saturniidae;
715 Cercophaninae). Entomo-Satsphingia 13: 4-78.
716 Breinholt J.W., Earl C., Lemmon A.R., Lemmon E.M., Xiao L., Kawahara A.Y. 2018.
717 Resolving relationships among the megadiverse butterflies and moths with a novel
718 pipeline for anchored phylogenomics. Syst. Biol. 67: 78-93.
719 Carrijo-Carvalho L.C., Chudzinski-Tavassi A.M. 2007. The venom of the *Lonomia*
720 caterpillar: an overview. Toxicon. 49: 741-757.
721 Chaimanee Y., Chavasseau O., Beard K.C., Kyaw A.A., Soe A.N., Sein C., Lazzari V.,
722 Marivaux L., Marandat B., Swe M., Rugbumrung M., Lwin T., Valentin X., MAung-

723 Thein Z.-M., Jaeger J.-J. 2012. Late Middle Eocene primate from Myanmar and the
724 initial anthropoid colonization of Africa. PNAS. 109: 10293-10297.
725 Chazot N., Condamine F.L., Dudas G., Pena C., Kodandaramaiah U., Matos-Maravi P.,
726 Aduse-Poku K., Elias M., Warren A.D., Lohmman D.J., Penz C.M, DeVries P., Zdenek
727 F.F., Nylin S., Müller C., Kawahara A.Y., Silva-Brandao K.L., Lamas G., Kleckova I.,
728 Zubek A., Ortiz-Acevedo E., Vila R., Vane-Wright R.I., Mullen S.P., Jiggins C.D.,
729 Wheat C.W., Freitas A.V.L., Wahlberg N. 2021. Conserved ancestral tropical niche but
730 different continental histories explain the latitudinal diversity gradient in brush-footed
731 butterflies. Nat. Commun. 12: 5717.
732 Chen D.B., Zhang R.S., Jin X.D., Yang J., Li P., Liu Y.Q. 2021. First complete mitochondrial
733 genome of *Rhodinia* species (Lepidoptera: Saturniidae): genome description and
734 phylogenetic implication. Bull. Entomol. Res.: 1-10.
735 Ciminera M., Auger-Rozenberg M.A., Caron H., Herrera M., Scotti-Saintagne C., Scotti I., N.
736 T., Roques A. 2018. Genetic variation and differentiation of *Hylesia metabus*
737 (Lepidoptera: Saturniidae): Moths of public health importance in French Guiana and in
738 Venezuela. J. Med. Entomol. 56: 137-148.
739 Condamine F.L., Sperling F.A., Wahlberg N., Rasplus J.-Y., Kergoat G.J. 2012. What causes
740 latitudinal gradients in species diversity? Evolutionary processes and ecological
741 constraints on swallowtail biodiversity. Ecol. Lett. 15: 267-277.
742 Cornee J.J., Munch P., Philippon M., BouDagher-Fadel M., Quillevere F., Melinte-
743 Dobrinescu M., Lebrun J.F., Gay A., Meyer S., Montheil L., Lallemand S., Marcaillou
744 B., Laurencin M., Legendre L., Garrocq C., Boucard M., Beslier M.-O., Laigle M.,
745 Schenini L., Fabre P.-H., Antoine P.-O., Marivaux L. 2021. Lost islands in the northern
746 Lesser Antilles: possible milestones in the Cenozoic dispersal of terrestrial organisms
747 between South America and the Greater Antilles. Earth-Sci. Rev. 217: 103617.

748 Coster P.M.C., Beard K.C., Salem M.J., Chaimanee Y., Jaeger J.-J. 2015. New fossils from
749 the Paleogene of central Libya illuminate the evolutionary history of endemic African
750 anomaluroid rodents. Front. Earth Sci. 3: 00056.
751 Cruaud A., Delvare G., Nidelet S., Sauné L., Ratnasingham S., Chartois M., Blaimer B.B.,
752 Gates M., Brady S.G., Faure S., van Noort S., Rossi J.-P., Rasplus J.-Y. 2021. Ultra-
753 Conserved Elements and morphology reciprocally illuminate conflicting phylogenetic
754 hypotheses in Chalcididae (Hymenoptera, Chalcidoidea). Cladistics. 37: 1-35.
755 Cruaud A., Nidelet S., Arnal P., Weber A., Fusu L., Gumovsky A., Huber J., Polaszek A.,
756 Rasplus J.-Y. 2019. Optimised DNA extraction and library preparation for small
757 arthropods: application to target enrichment in chalcid wasps used for biocontrol. Mol.
758 Ecol. Resour. 19: 702-710.
759 Davis R. B., Javois J., Kaasik A., Ounap E., Tammaru T. 2016. An ordination of life histories
760 using morphological proxies: capital vs. income breeding in insects. Ecology. 97: 2112-
761 2124.
762 Dong Y., Dai F.Y., Ren Y.D., Liu H., Chen L., Yang P.C., Liu Y.Q., Li X., Wang W., Xiang
763 H. 2015. Comparative transcriptome analyses on silk glands of six silkmoths imply the
764 genetic basis of silk structure and coloration. BMC Genomics. 16: 203.
765 Duchêne D., Mather N., Van Der Wal C., Ho S. 2021. Excluding loci with substitution
766 saturation improves inferences from phylogenomic data. Syst. Biol. Syab075.
767 Economo E.P., Narula N., Friedman N.R., Weiser M.D., Guénard B. 2018. Macroecology and
768 macroevolution of the latitudinal diversity gradient in ants. Nat. Comm. 9: 1778.
769 Faircloth B.C. 2017. Identifying conserved genomic elements and designing universal bait
770 sets to enrich them. Methods Ecol. Evol. 8: 1103-1112.

771 Fogang Mba A.R., Kansci G., Viau M., Rougerie R., Genot C. 2019. Edible caterpillars of
772 *Imbrasia truncata* and *Imbrasia epimethea* contain lipids and proteins of high potential
773 for nutrition. J Food Compost Anal. 79: 70-79.
774 Garrocq C., Lallemand S., Marcaillou B., Lebrun J.F., Padron C., Klingelhoefer F., Laigle M.,
775 Munch P., Gay A., Schenini L., Beslier M.-O., Cornee J.-J., Mercier de Lépinay B.,
776 Quillévéré F., Boudagher-fadel M. 2021. Genetic relations between the Aves Ridge and
777 the Grenada back-arc basin, East Caribbean sea. J. Geophys. Res. Solid Earth. 126:
778 e2020JB020466.
779 Guindon S., Dufayard J.F., Lefort V., Anisimova M., Hordijk W., Gascuel O. 2010. New
780 algorithms and methods to estimate maximum-likelihood phylogenies: assessing the
781 performance of PhyML 3.0. Syst. Biol. 59: 307-321.
782 Hamilton C., St Laurent R., Dexter K., Kitching I., Breinholt J., Zwick A., Timmermans M.,
783 Barber J., Kawahara A. 2019. Phylogenomics resolves major relationships and reveals
784 significant diversification rate shifts in the evolution of silk moths and relatives. BMC
785 Evol. Biol. 19: 182.
786 Hamilton C.A., Winiger N., Rubin J.J., Breinholt J., Rougerie R., Kitching I.J., Barber J.R.,
787 Kawahara A.Y. 2021. Hidden phylogenomic signal helps elucidate arsenurine silkmoth
788 phylogeny and the evolution of body size and wing shape trade-offs. Syst. Biol.:
789 syab090.
790 Hartenberger J. 1998. An Asian Grande Coupure. Nature. 394: 321.
791 Harzhauser M., Kroh A., Mandic O., Piller W.E., Göhlich U., Reuter M., Berning B. 2007.
792 Biogeographic responses to geodynamics: A key study all around the Oligo-Miocene
793 Tethyan Seaway. Zool. Anz. 246: 241-256.

794 Huchon D., Chevret P., Jordan U., Kilpatrick C.W., Ranwez V., Jenkins P.D., Brosius J.,
795 Schmitz J. 2007. Multiple molecular evidences for a living mammalian fossil. PNAS.
796 104: 7495-7499.
797 Iturralde-Vinent M.A. 2006. Meso-Cenozoic Caribbean paleogeography: Implications for the
798 historical biogeography of the region. Int. Geol. Rev. 48: 791-827.
799 Ivanova N.V., Dewaard J.R., Hebert P.D.N. 2006. An inexpensive, automation-friendly
800 protocol for recovering high-quality DNA. Mol. Ecol. Notes. 6: 998-1002.
801 Jahren A.H. 2007. The Arctic Forest of the Middle Eocene. Annu. Rev. Earth Planet. Sci. 35:
802 509-540.
803 Jia D.-R., Bartish I.V. 2018. Climatic changes and orogeneses in the late Miocene of Eurasia:
804 The main triggers of an expansion at a continental scale? Front. Plant Sci. 9: 1400.
805 Kalyaanamoorthy S., Minh B.Q., Wong T.K.F., von Haeseler A., Jermiin L.S. 2017.
806 ModelFinder: fast model selection for accurate phylogenetic estimates. Nat. Methods.
807 14: 587-589.
808 Kassambara A. 2020. ggpubr: ggplot2 Based Publication Ready Plots. R package version
809 0.3.0 https://CRAN.R-project.org/package=ggpubr.
810 Katoh K., Standley D.M. 2013. MAFFT multiple sequence alignment software version 7:
811 improvements in performance and usability. Mol. Biol. Evol. 30: 772-780.
812 Kawahara A.Y., Plotkin D., Espeland M., Meusemann K., Toussaint E.F.A., Donath A.,
813 Gimnich F., Frandsen P.B., Zwick A., Reis dos M., Barber J.R., Peters R.S., Liu S.,
814 Zhou X., Mayer C., Podsiadlowski L., Storer C., Yack J.E., Misof B., Breinholt J.W.
815 2019. Phylogenomics reveals the evolutionary timing and pattern of butterflies and
816 moths. PNAS. 116: 22657–22663.

817 Kitching I.J., Rougerie R., Zwick A., Hamilton C.A., St Laurent R.A., Naumann S., Mejia
818 L.B., Kawahara A.Y. 2018. A global checklist of the Bombycoidea (Insecta:
819 Lepidoptera). BDJ. 6: e22236.
820 Klaus K.V., Matzke N.J. 2020. Statistical comparison of trait-dependent biogeographical
821 models indicates that Podocarpaceae dispersal is influenced by both seed cone traits and
822 geographical distance. Syst. Biol. 69: 61–75.
823 Kozlov A.M., Darriba D., Flouri T., Morel B., Stamatakis A. 2019. RAxML-NG: a fast,
824 scalable and user-friendly tool for maximum likelihood phylogenetic inference.
825 Bioinformatics, 35: 4453-4455.
826 Kumar S., Filipski A.J., Battistuzzi F.U., Pond S.L.K., Tamura K. 2012. Statistics and truth in
827 phylogenomics. Mol. Biol. Evol. 29: 457-472.
828 Kundu S.C., Kundu B., Talukdar S., Bano S., Nayak S., Kundu J., Mandal B.B., Bhardwaj N.,
829 Botlagunta M., Dash B.C., et al. 2012. Invited review nonmulberry silk biopolymers.
830 Biopolymers. 97: 455-467.
831 Landis M., Matzke N., Moore B., Huelsenbeck J. 2013. Bayesian analysis of biogeography
832 when the number of areas is large. Syst. Biol. 62: 789-804.
833 Lanfear R., Frandsen P.B., Wright A.M., Senfeld T., Calcott B. 2017. PartitionFinder 2: New
834 methods for selecting partitioned models of evolution for molecular and morphological
835 phylogenetic analyses. Mol. Biol. Evol. 34: 772-773.
836 Lemaire C. 2002. The Saturniidae of America. Vol. 4. Hemileucinae. 1388 pp. Goecke &
837 Evers Eds., Keltern, Germany.
838 LePage B., Yang H., Matsumoto M. 2005. The Evolution and biogeographic history of
839 Metasequoia. In: LePage B., Williams C.J., Yang H. eds. The Geobiology and Ecology
840 of Metasequoia. Dordrecht, The Netherlands, Springer: 3-114.

841 Licht A., Métais G., Coster P., İbilioğlu D., Ocakoğlu F., Westerweel J., Mueller M.,
842 Campbell C., Mattingly S., Wood M.C., Beard K.C. 2022. Balkanatolia: The insular
843 mammalian biogeographic province that partly paved the way to the Grande Coupure.
844 Earth Sci. Rev. 226: 103929.
845 Maechler M., Rousseeuw P., Struyf A., Hubert M., Hornik K. 2018. cluster: Cluster Analysis
846 Basics and Extensions. R package version 2.0.7-1.
847 Mai U., Mirarab S. 2018. TreeShrink: fast and accurate detection of outlier long branches in
848 collections of phylogenetic trees. BMC Genomics. 19: 272.
849 Marivaux L., Essid E.M., Marzougui W., Ammar H.K., Adnet S., Marandat B., Merzeraud
850 G., Tabuce R., Vianey-Liaud M. 2014. A new and primitive species of *Protophiomys*
851 (Rodentia, Hystricognathi) from the late middle Eocene of Djebel el Kébar, central
852 Tunisia. Palaeovertebrata. 38: e2.
853 Matzke N. 2014. Model selection in historical biogeography reveals that founder-event
854 speciation is a crucial process in island clades. Syst. Biol. 63: 951-970.
855 Matzke N.J. 2021. Statistical comparison of DEC and DEC+J is identical to comparison of
856 two ClaSSE submodels, and is therefore valid. OSF Preprints.
857 Michener C.D. 1952. The Saturniidae (Lepidoptera) of the western hemisphere: morphology,
858 phylogeny and classification. Bull. Am. Mus. Nat. Hist., 98: 341–501.
859 Minet J. 1994. The Bombycoidea phylogeny and higher classification (Lepidoptera,
860 Glossata). Insect. Syst. Evol. 25: 63-88.
861 Minh B., Hahn M., Lanfear R. 2020 New methods to calculate concordance factors for
862 phylogenomic datasets. Mol. Biol. Evol. 37: 2727-2733.
863 Minh B.Q., Nguyen M.A.T., von Haeseler A. 2013. Ultrafast approximation for phylogenetic
864 bootstrap. Mol. Biol. Evol. 30: 1188-1195.

865 Minh B.Q., Schmidt H.A., Chernomor O., Schrempf D., Woodhams M.D., von Haeseler A.,
866 Lanfear R. 2020. IQ-TREE 2: New models and efficient methods for phylogenetic
867 inference in the genomic era. Mol. Biol. Evol. 37: 1530-1534.
868 Mirarab S., Nguyen N., Guo S., Wang L.S., Kim J., Warnow T. 2015. PASTA: Ultra-Large
869 Multiple Sequence Alignment for Nucleotide and Amino-Acid Sequences. J. Comput.
870 Biol. 22: 377-386.
871 Morley R.J. 2003. Interplate dispersal paths for megathermal angiosperms. Perspect. Plant
872 Ecol. Evol. Syst. 6: 5-20.
873 Morley R.J. 2011. Cretaceous and Tertiary climate change and the past distribution of
874 megathermal rainforests. In Tropical Rainforest Responses to Climatic Change. Eds.
875 Bush M., Flenley J., Gosling W. Springer-Verlag, Berlin Heidelberg, Germany: 1-34.
876 Nässig W.A. 1991. Biological observations and taxonomic notes on *Actias isabellae* (Graells)
877 (Lepidoptera, Saturniidae). Nota lep. 14: 131-143.
878 Nässig W.A., Naumann S., Oberprieler R.G. 2015. Notes on the Saturniidae of the Arabian
879 Peninsula, with description of a new species (Lepidoptera: Saturniidae). Nachr.
880 Entomol. Ver. Apollo, N.F. 36: 31-38.
881 Nguyen L.T., Schmidt H.A., von Haeseler A., Minh B.Q. 2015. IQ-TREE: A fast and
882 effective stochastic algorithm for estimating maximum likelihood phylogenies. Mol.
883 Biol. Evol. 32: 268-274.
884 Oberprieler R.G., Nässig W.A. 1994. Tarn- oder Warntrachten - ein Vergleich larvaler und
885 imaginaler Strategien bei Saturniinen (Lepidoptera: Saturniinen). Nachr. Entomol. Ver.
886 Apollo, N.F. 15: 267-303.
887 Oberprieler R.G. 1997. Classification of the African Saturniidae (Lepidoptera) - The quest for
888 natural groups and relationships. Metamorphosis. Suppl. 3: 142-155.

889 Paradis E., Schliep K. 2018. ape 5.0: an environment for modern phylogenetics and
890 evolutionary analyses in R. Bioinformatics 35: 526-528.
891 Philippe H., Brinkmann H., Lavrov D., Littlewood D., Manuel M., Wörheide G., Baurain D.
892 2001. Resolving difficult phylogenetic questions: why more sequences are not enough.
893 PLoS Biol. 9: e1000602.
894 Philippon M., Cornee J.J., Munch P., van Hinsbergen D.J.J., BouDagher-Fadel M., Gailler L.,
895 Boschman L.M., Quillevere F., Montheil L., Gay A., Lebrun J.F., Lallemand S.,
896 Marivaux L., Antoine P.-O. 2020. Eocene intra-plate shortening responsible for the rise
897 of a faunal pathway in the northeastern Caribbean realm. PLoS One. 15: e0241000.
898 Pindell J., Kennan L., Maresch W.V., Stanek K., Draper G., Higgs R. 2005. Plate-kinematics
899 and crustal dynamics of circum-Caribbean arc-continent interactions: tectonic controls
900 on basin development in Proto-Caribbean margins. Geological Society of America
901 Special Paper, 394: 7–52.
902 R Core Team. 2018. R version 3.5.1 (Feather Spray): A language and environment for
903 statistical computing. R Foundation for Statistical Computing, Vienna, Austria. URL
904 https://www.R-project.org/.
905 Rambaut A., Drummond A., Xie D., Baele G., MA S. 2018. Posterior summarization in
906 Bayesian phylogenetics using Tracer 1.7. Syst. Biol. 67: 901-904.
907 Rasplus J.-Y., Rodriguez L.J., Sauné L., Peng Y.-Q., Bain A., Kjellberg F., Harrison R.D.,
908 Pereira R.A.S., Ubaidillah R., Tollon-Cordet C., Gautier M., Rossi J.-P., Cruaud A.
909 2021. Exploring systematic biases, rooting methods and morphological evidence to
910 unravel the evolutionary history of the genus *Ficus* (Moraceae). Cladistics. 37: 402-422.
911 Ree R., Sanmartin I. 2018. Conceptual and statistical problems with the DEC+J model of
912 founder□event speciation and its comparison with DEC via model selection. J.
913 Biogeogr. 45: 741-749.

914 Ree R.H., Smith S.A. 2008. Maximum-likelihood inference of geographic range evolution by
915 dispersal, local extinction, and cladogenesis. Syst. Biol. 57: 4-14.
916 Regier J.C., Cook C.P., Mitter C., Hussey A. 2008. A phylogenetic study of the 'bombycoid
917 complex' (Lepidoptera) using five protein-coding nuclear genes, with comments on the
918 problem of macrolepidopteran phylogeny. Syst. Ent. 33: 175-189.
919 Regier J.C., Mitter C., Peigler R.S., Friedlander T.P. 2002. Monophyly, composition, and
920 relationships within Saturniinae (Lepidoptera : Saturniidae): Evidence from two nuclear
921 genes. Insect. Syst. Evol. 33: 9-21.
922 Robinson D., Foulds L. 1981. Comparison of phylogenetic trees. Math. Biosci. 53: 131-147.
923 Rogl F. 1999. Mediterranean and Paratethys. Facts and hypotheses of an Oligocene to
924 Miocene paleogeography (short overview). Geol. Carpath. 50: 339-349.
925 Romiguier J., Cameron S.A., Woodard S.H., Fischman B.J., Keller L., Praz C.J. 2016.
926 Phylogenomics controlling for base compositional bias reveals a single origin of
927 eusociality in corbiculate bees. Mol. Biol. Evol. 33: 670-678.
928 Romiguier J., Roux C. 2017. Analytical biases associated with GC-content in molecular
929 evolution. Front. Genet. 8: 00016.
930 Ronquist F. 1997. Dispersal-vicariance analysis: a new approach to the quantification of
931 historical biogeography. Syst. Biol. 46: 195-203.
932 Rossi J.-P. 2011. rich: an R package to analyse species richness. Diversity. 3: 112-120.
933 Rougerie R. 2005. Phylogeny and biogeography of the Saturniinae (Lepidoptera:
934 Bombycoidea, Saturniidae). PhD Thesis. Muséum National d'Histoire Naturelle, Paris,
935 France: 530 pp + 45 pl.
936 Rubin J.J., Hamilton C.A., McClure C.J.W., Chadwell B.A., Kawahara A.Y., Barber J.R.
937 2018. The evolution of anti-bat sensory illusions in moths. Sci. Adv. 4: eaar7428.

938 Rubinoff D., Doorenweerd C. 2020. In and out of America: Ecological and species diversity
939 in Holarctic giant silkmoths suggests unusual dispersal, defying the dogma of an Asian
940 origin. J. Biogeogr. 47: 903-914.
941 Shimodaira H. 2002. An approximately unbiased test of phylogenetic tree selection. Syst.
942 Biol. 51: 492-508.
943 Shimodaira H., Hasegawa M. 2001. CONSEL: for assessing the confidence of phylogenetic
944 tree selection. Bioinformatics 17: 1246-1247.
945 Smith P., Rios S., Atkinson K., Mielke O., Casagrande M. 2013. New Paraguayan specimens
946 and first confirmed phenological data for *Catharisa cerina* Jordan 1911 (Lepidoptera:
947 Saturniidae). Rev. Bras. Biocienc. 11: 349-351.
948 Sohn J.C., Labandeira C., Davis D., Mitter C. 2012. An annotated catalog of fossil and
949 subfossil Lepidoptera (Insecta: Holometabola) of the world. Zootaxa 3286:1-116.
950 Sota T., Takami Y., Ikeda H., Liang H., Karagyan G., Scholtz C., Hori M. 2022. Global
951 dispersal and diversification in ground beetles of the subfamily Carabinae. Mol.
952 Phylogenet. Evol. 167: 107355.
953 Stamatakis A. 2014. RAxML version 8: a tool for phylogenetic analysis and post-analysis of
954 large phylogenies. Bioinformatics 30: 1312-1313.
955 Struck T.H. 2014. TreSpEx - Detection of misleading signal in phylogenetic reconstructions
956 based on tree information. Evol. Bioinform. Online. 10:51-67.
957 Tagliacollo V.A., Lanfear R., Townsend J. 2018. Estimating Improved Partitioning Schemes
958 for Ultraconserved Elements. Mol. Biol. Evol. 35: 1798-1811.
959 Vandenberghe N., Hilgen F.J., Speijer R.P. 2012. Chapter 28. The Paleogene Period. In:
960 Gradstein F.M., Ogg J.G., Schmitz M.D., Ogg G.M. eds. The Geologic Time Scale.
961 Elsevier: 855-921.

962 Westerhold T., Marwan N., Drury A.J., Liebrand D., Agnini C., Anagnostou E., Barnet
963 J.S.K., Bohaty S.M., De Vleeschouwer D., Florindo F., Frederichs T., Hodell D.A.,
964 Holbourn A.E., Kroon D., Lauretano V., Littler K., Lourens L.J., Lyle M., Palike H.,
965 Rohl U., Tian J. Wilkens R.H., Wilson P.A., Zachos J.C. 2020. An astronomically dated
966 record of Earth's climate and its predictability over the last 66 million years. Science.
967 369: 1383-1387.
968 Xing Y., Ree R.H. 2017. Uplift-driven diversification in the Hengduan Mountains, a
969 temperate biodiversity hotspot. PNAS. 114: E3444-E3451.
970 Yang Z., Rannala B. 2006. Bayesian estimation of species divergence times under a
971 molecular clock using multiple fossil calibrations with soft bounds. Mol. Biol. Evol.,
972 23: 212-226.
973 Yang J., Wang Y.-F., Spicer R.A., Mosbrugger V., Li C.-S., Sun Q.-G. 2007. Climatic
974 Reconstruction at the Miocene Shanwang Basin, China, Using Leaf Margin Analysis,
975 CLAMP, Coexistence Approach, and Overlapping Distribution Analysis. Am. J. Bot.
976 94: 599-608.
977 Zhang C., Rabiee M., Sayyari E., Mirarab S. 2018. ASTRAL-III: polynomial time species
978 tree reconstruction from partially resolved gene trees. BMC Bioinformatics. 19: 153.
979 Zhang J., Sun B., Zhang X.J. 1994. Miocene Insects and Spiders from Shanwang, Shandong.
980 Beijing, China. Beijing Science Press. v + 298 pp.
981 Zhong B., Betancur-R R. 2017. Expanded taxonomic sampling coupled with gene genealogy
982 interrogation provides unambiguous resolution for the evolutionary root of
983 angiosperms. Genome Biol. Evol. 9: 3154-3161.
984 Zhu Q. 2014. AfterPhylo. A Perl script for manipulating trees after phylogenetic
985 reconstruction. Available from https://github.com/qiyunzhu/AfterPhylo/.
986

Author Contributions

Designed the study: AC, JYR, PA, RR

Obtained funding: AC, CLV, FLC, JM, JYR, ME, RR, SL, TD

Contributed samples: CLV, JYR, PDNH, RR, TD

Identified samples: IJK, JYR, RR, TD

Performed laboratory work: AC, DG, JYR, PA, RR, SN, YC

Analyzed data: AC, JYR, PA, RR

Discussed results: AC, CLV, FLC, IJK, JM, JYR, LBM, ME, PA, RR, SL, TD

Drafted the manuscript: AC, JYR, PA, RR

All authors commented on the manuscript

Data Availability

Fastq paired reads for analyzed samples are available as a NCBI Sequence Read Archive (ID#PRJNA XXXXX). Custom script for random sampling of sites within data sets is available from https://github.com/acruaud/saturniidae_phylogenomics_2022. Data sets (concatenated UCEs) and trees have been uploaded on Dryad (http://dx.doi.org/10.5061/dryad.[NNNN]).

TABLE AND FIGURE LEGENDS

Table 1. Summary of mean divergence time estimates and 95% highest posterior density (HPD) for groups or colonization events discussed. Mean and median ages with 95% HPD for all nodes are provided in Table S4. Units are in Myr. Our new classification is used for taxon names. ACH = Arsenurinae + Ceratocampinae + Hemileucinae; BSS = Bunaeinae + Salassinae + Saturniinae.

Figure 1. Conflicting topologies observed after analysis of the initial data set (a) and results of the gene genealogy interrogation (GGI) approach (b). In panel (a), topology *A* is supported by IQ-TREE analyses; *Abis* is supported by ASTRAL90; *B* is supported by ASTRAL70 and *C* is supported by ASTRAL50. All corresponding trees are available in Figure S1. In simplified topologies, Hemileucinae is used for Hemileucinae minus *Hirpida* and *Hirpsinjaevia* and Hirpi/Hirpsi stands for *Hirpida* + *Hirpsinjaevia.* For the GGI approach, Hemileucinae (minus *Hirpida* and *Hirpsinjaevia*) + Ceratocampinae + Arsenurinae; Saturniinae + Salassinae; *Hirpida* + *Hirpsinjaevia* and Agliinae were considered as different clades and trees were inferred using each of the competing topologies as multifurcating constraint trees. The structure of the backbone was fixed, but taxa within clades were free to move around. Topology *A* was considered equivalent to *Abis* as we focused on sister taxa relationships of Agliinae / *Hirpida* + *Hirpsinjaevia* with either Hemileucinae + Ceratocampinae + Arsenurinae or Saturniinae + Salassinae. In panel (b), average values of GC content and saturation (R-squared of the regression between pairwise distances calculated from aligned sequences and branch length) for loci that significantly supported topologies *A*/*Abis* (i.e., Pvalue of the AU test ≦ 0.05; N loci = 189; Table S3) or not (Nloci=796) were compared using a randomization test (N randomization = 9999; c2m function of the R package *rich*) and P values are reported on graph.

Figure 2. Saturniidae tree of life. The classification proposed in this study is mapped on the chronogram (MCMCtree, uncorrelated relaxed clock model) inferred from the topology selected after exploration of systematic bias (i.e., the IQ-TREE tree inferred from the 50% least saturated loci). Red dots at nodes identify poorly supported nodes (SHaLRT<80 or UFBoot<95). Abbreviations used: A = Antistathmopterini; Agl = Agliinae; Al = Almeidaiini; Bathy = Bathyphlebiini; C = Cercophanini; Cer = Cercophaninae; Cith = Citheroniini; E = Eudaemoniini; Eo = Eochroini; Hir = Hirpidinae; J = Janiodini; Lono = Lonomiini; Oxyteninae; P = Pseudapheliini; Poly = Polythysanini; Sal = Salassinae; So = Solini; Urot = Urotini.

Figure 3. Global historical biogeography of Saturniidae. Ancestral ranges were inferred with the BAYAREALIKE+J model (best-fit and most plausible model according to empirical considerations; see text) as implemented in *BioGeoBEARS*. Alternative inferences of ancestral ranges are provided in Figure S5. The chronogram is derived from the species-level chronogram obtained with the uncorrelated relaxed clock model implemented in MCMCtree (see Fig. 2) that was pruned to keep only one specimen per genus/subgenus. The classification proposed in this study is used to annotate the tree. Colored boxes following each terminal name represent biogeographical regions A to I as illustrated in the upper-left map; colored arrows refer to inferred dispersal/colonization events. Abbreviations used: A = Agliinae; Ars = Arsenurinae; C=Cercophaninae; H = Hirpidinae; O = Oxyteninae; S = Salassinae. PPH=Pliocene, Pleistocene and Holocene. Illustrative photograph = *Antherina suraka* (Saturniinae); image courtesy of Armin Dett.